Journal of Hazardous Materials 179 (2010) 309–317

Contents lists available at ScienceDirect

Journal of Hazardous Materials

journal homepage: www.elsevier.com/locate/jhazmat

Thermodynamic modelling of the formation of zinc–manganese ferrite spinel in electric arc furnace dust

C.A. Pickles*

Robert M. Buchan Department of Mining, Queen's University, Kingston, Ontario, K7L-3N6, Canada

ARTICLE INFO

Article history:
Received 14 December 2009
Received in revised form 26 February 2010
Accepted 1 March 2010
Available online 7 March 2010

Keywords:
Electric arc furnace dust
Zinc–manganese ferrite
Zinc
Spinel
Thermodynamics
Modelling

ABSTRACT

Electric arc furnace dust is generated when automobile scrap, containing galvanized steel, is remelted in an electric arc furnace. This dust is considered as a hazardous waste in most countries. Zinc is a major component of the dust and can be of significant commercial value. Typically, the majority of the zinc exists as zinc oxide (ZnO) and as a zinc–manganese ferrite spinel ($(Zn_xMn_yFe_{1-x-y})Fe_2O_4$). The recovery of the zinc from the dust in metal recycling and recovery processes, particularly in the hydrometallurgical extraction processes, is often hindered by the presence of the mixed ferrite spinel. However, there is a paucity of information available in the literature on the formation of this spinel. Therefore, in the present research, the equilibrium module of HSC Chemistry® 6.1 was utilized to investigate the thermodynamics of the formation of the spinel and the effect of variables on the amount and the composition of the mixed ferrite spinel. It is proposed that the mixed ferrite spinel forms due to the reaction of iron–manganese particulates with both gaseous oxygen and zinc, at the high temperatures in the freeboard of the furnace above the steel melt. Based on the thermodynamic predictions, methods are proposed for minimizing the formation of the mixed ferrite spinel.

1. Introduction

During the remelting of automobile scrap, containing galvanized steel, in an electric arc furnace (EAF) a dust is produced as a result of the simultaneous evaporation and oxidation of the various metals, ejection of particulates from the metal and slag and also via the entrapment of low-density furnace additives [1–3]. This EAF dust represents about 1–2% of the furnace charge and can contain substantial amounts of zinc, iron and calcium oxides as well as numerous other metals and non-metals. The non-ferrous metals in the dust can be of significant commercial value. In most countries the dust is considered as a hazardous waste because of the presence of leachable lead, zinc, cadmium and chromium. There are two major approaches for dealing with the dust [4–6]: (1) stabilization followed by disposal or (2) processing for the recovery of the valuable metals. In either case, the speciation of the zinc and the other metals can influence their behavior during these treatment methods and could have detrimental effects on either the metal recovery or the process itself. Therefore, in order to control or prevent their formation, it is important to determine the conditions under which these species can develop during the dust formation process. In general, the dust composition will depend on the scrap composition, the gas composition in the freeboard of the furnace, the operating parameters of the furnace and the conditions in the off-gas handling system.

There have been a large number of studies on the characterization of EAF dust and each dust is site-specific [7–14]. However, the zinc in the dust typically exists as zinc oxide (ZnO) and as a mixed zinc–manganese ferrite spinel or ZMFO ($(Zn_xMn_yFe_{1-x-y})Fe_2O_4$). In the automotive scrap, the zinc is mainly present as a coating on the galvanized steel and since the boiling point of zinc (1180 K) is less than the typical operating temperature of the steelmaking process (1873 K), then the zinc will evaporate and enter the gas phase in the freeboard of the furnace. Additionally, some iron (boiling point of 3134 K) will enter the gas phase either by direct evaporation or indirectly by the bursting of gas bubbles [15]. In the furnace atmosphere, the iron can form either iron oxides or the iron, zinc and oxygen can react to form zinc ferrite ($ZnFe_2O_4$). Only a few thermodynamic studies have been performed on the formation of zinc ferrite in EAF dust [16–18]. However, at the high temperatures in the atmosphere of an electric arc furnace, the zinc and iron are usually not present as zinc ferrite but in combination with other metals such as manganese as ZMFO. Most commercial automotive steels contain a relatively small percentage of manganese (0.3–0.8%). Since the boiling point of manganese (2335 K) is significantly lower than that of iron (3134 K) and iron–manganese liquid solutions are close to ideal then a significant amount of the manganese will evaporate. Manganese is about one hundred to one

* Tel.: +1 613 533 2759; fax: +1 613 533 6597.
E-mail address: pickles-c@mine.queensu.ca.

0304-3894/$ – see front matter © 2010 Elsevier B.V. All rights reserved.
doi:10.1016/j.jhazmat.2010.03.005

thousand times more volatile than iron in the temperature range of 1673–2373 K [19]. As a result, the manganese to iron ratio of the dust can be significantly higher than that of the steel [20]. Typical EAF dusts can contain manganese concentrations upto about 5%. In general, the behavior of the manganese in the dust is similar to that of the iron, and manganese can be found as manganese oxide but it can also substitute for iron in the ZMFO. Therefore, the presence of some manganese can affect both the formation and the composition of the ferrite spinel.

The composition of the gas in the furnace atmosphere can have a significant effect on the dust composition. Typically, the major gaseous constituents of the electric arc furnace atmosphere are: nitrogen (N_2), oxygen (O_2), carbon monoxide (CO), carbon dioxide (CO_2), hydrogen (H_2) and water vapour (H_2O). The minor constituents would be as follows: sulphur dioxide (SO_2), sulphur trioxide (SO_3), vapourised hydrocarbons (C_xH_y), ozone (O_3), nitrous oxides (NO_x), hydrogen sulphide (H_2S), hydrogen chloride (HCl), hydrogen fluoride (HF), silicon tetrafluoride (SiF_4), ammonia (NH_3) and dioxins ($C_{12}H_{8-x}Cl_xO_2$). The presence of significant amounts of carbon monoxide and carbon dioxide will depend on whether the conditions in the furnace are reducing or oxidizing. In the past, reducing conditions were achieved by adding carbon to the slag and this increased the amount of carbon monoxide in the furnace atmosphere and ultimately, the amount of carbon dioxide in the off-gas. Furthermore, the recent introduction of alternative fuel sources, such as oxy-fuel burners has resulted in increased amounts of carbon monoxide and hydrogen in the furnace atmosphere [21]. This additional carbon dioxide and water vapour in the off-gas can promote the formation of hydrated and carbonated species in the dust. Again because of the presence of considerable water and carbon dioxide in the off-gas, the zinc-containing species could be carbonated and/or hydrated.

In this research, the formation of ZMFO in EAF dust in a simulated gas composition was studied using the Equilibrium Module of HSC Chemistry® 6.1. The effects of temperature, the amounts of zinc, manganese and iron in the dust, the oxygen potential, the dust loading and the calcium oxide content of the dust were investigated. The conditions for minimizing the formation of ZMFO are elucidated and a possible formation mechanism is discussed.

2. Thermodynamic calculations

The equilibrium amounts of the various species were calculated using the Equilibrium Module of HSC Chemistry® 6.1 [22]. For any given reaction system, the various phases and species that are known to be present are specified and the input consists of the amounts of the reacting species. Then the calculations are performed at the specified temperature and pressure and the equilibrium amounts of the products are calculated using the Gibbs free energy minimization method. Ideal mixing of a species in a solution is assumed and the activity coefficients are taken to be unity, unless values for the activity coefficients have been inputted. Kinetic effects can be taken into account by deleting species, which would not be expected to form under the selected conditions. The major variables studied were: the dust loading (mg of dust/m^3 of gas), the composition of the solids in the off-gas, the composition of the off-gas and the temperature of the off-gas during cooling.

If specific data for a given species is not available in the HSC database then it can either be added if it exists or it can be approximated. Although the thermodynamic properties of zinc ferrite ($ZnFe_2O_4$) are well-established, there is no available thermodynamic data for ZMFO ($(Zn_xMn_yFe_{1-x-y})Fe_2O_4$). The general spinel ferrite (MFe_2O_4, where M = Zn, Mn or Fe) can be described as a cubic close-packed structure consisting of oxygen ions, with M^{2+} ions having tetrahedral oxygen coordination and the Fe^{3+} ions having octahedral oxygen coordination. This mixed spinel can be considered to be a mixture of zinc ferrite ($ZnFe_2O_4$), manganese ferrite ($MnFe_2O_4$) and magnetite (Fe_3O_4) and in the calculations it was assumed to be a separate phase with ideal mixing. In this study, the composition of the spinel was represented in terms of the percentages of $ZnFe_2O_4$, $MnFe_2O_4$ and Fe_3O_4 or in terms of the amounts of zinc (x), manganese (y) or iron ($1-x-y$).

The furnace atmosphere was assumed to consist of mainly carbon monoxide, hydrogen, carbon dioxide, water vapour, oxygen and nitrogen. Measurements of the off-gas composition from various electric arc furnaces have given the following typical concentrations in the temperature range of 1300–1600 K [23]; carbon monoxide in the range of 15–20% with values as high as 40%, hydrogen contents of 10–20% with values as high as 35%, carbon dioxide in the range of 20–25% with values as high as 35% and water vapour contents upto 30%. The balance of the off-gas is mainly oxygen and nitrogen. The control atmosphere in this study at 1600 K was assumed to consist of 100 mol of gas with the following composition: 20.14%CO_2, 15.18%N_2, 11.34%H_2, 23.89%H_2O, 29.45%CO, 2.68×10^{-7}%CH_4 and 1.99×10^{-8}%O_2. As the temperature decreases, increasing amounts of both water vapour and carbon dioxide are formed and as room temperature is approached then the water vapour condenses. At room temperature, i.e. 298 K, the gas composition would be: 63.75%CO_2, 33.09%N_2, 1.25×10^{-5}%H_2, 3.15%H_2O, 2.45×10^{-9}%CO, 1.11×10^{-3}%CH_4 and 2.21×10^{-36}%O_2. The amount of gas would be 46.74 kmol plus 33.09 kmol of liquid water and 20.17 kmol of solid carbon for a total of 100 kmol. In an electric arc furnace operation there could be supplementary air in the furnace as a result of post-combustion and/or the deliberate addition of air for cooling purposes. In order to simulate more closely the gas composition in equilibrium with the dust, a further 100 mol of air (79%N_2 and 21%O_2) was added at 1600 K. At room temperature, the standard gas composition would be: 33.26%CO_2, 63.17%N_2, 1.00×10^{-34}%H_2, 3.16%H_2O, 1.00×10^{-34}%CO, 1.00×10^{-34}%CH_4 and 0.41%O_2. There would be 169.49 mol of gas and 30.51 mol of liquid water and a negligible amount of solid carbon.

Another possible controlling factor with regards to the dust composition is the dust loading in the furnace atmosphere, which can be as high as 100 g/m^3 during oxygen injection [24,25]. On the other hand, the discharge dust loading, which is generally subject to government regulations, can be lower than 100 mg/m^3 [26]. However, there is a paucity of information on the typical dust loading in an off-gas handling system. In order to ensure that there was an excess of gas to react with the dust in the calculations, then the discharge dust loading values were utilized. For 200 kmol of gas, for a zinc to iron molar ratio of 3:1 and assuming that the amounts of zinc, iron and manganese available to form the dust are 3×10^{-4}, 1×10^{-4} and 0.5×10^{-4} kmol, respectively, then this gives a dust loading of the order of about 10 mg/m^3.

3. Equilibrium calculations for the Zn–Fe–Mn–O–H–C system

3.1. Effect of temperature

It is likely that the zinc ferrite spinel type phases such as ZMFO form at the high temperatures in the freeboard of the furnace [16–18]. In the early stages of the steelmaking process the major components arising from the scrap would be zinc, iron and manganese. Inputting zinc, iron, manganese, oxygen, hydrogen and carbon into the Equilibrium Module of HSC Chemistry® 6.1 generates a list of 188 species, many of which would be considered unstable under the operating conditions. Therefore, these unstable species were deleted and the six phases and the 42 species utilized

Table 1
Phases (six) and species (42) utilized in the equilibrium calculations.

Phase 1: Gases	Phase 2: Oxides	Phase 2: Oxides	Phase 4: Metal
N_2	$FeCO_3$	$ZnC_2O_4{\cdot}H_2O$	Fe
CH_4	FeO	ZnO	Mn
CO	Fe_2O_3	$Zn(OH)_2$	Zn
CO_2	$Fe(OH)_2$	$Zn_5(OH)_6(CO_3)_2$	
O_2	$Fe(OH)_3$		
Fe	$Fe_2O_3{\cdot}H_2O$		Phase 5: Water
FeO	FeO·OH		H_2O
FeO_2	$MnCO_3$	Phase 3: Spinel	
H_2	MnO	Fe_2MnO_4	
H_2O	MnO_2	$ZnFe_2O_4$	Phase 6: Carbon
Mn	Mn_2O_3	Fe_3O_4	C
MnO	Mn_3O_4		
MnO_2	$Mn(OH)_2$		
Zn	MnO·OH		
ZnO	$ZnCO_3$		

in the calculations are shown in Table 1. The behavior of the zinc-containing species as a function of temperature is shown in Fig. 1. Metallic zinc vapour and a small amount of gaseous zinc oxide are the most significant species at high temperatures and the ZMFO begins to form at about 1900 K and generally the amount increases with decreasing temperature. As the temperature decreases even further, then some of the zinc vapour is replaced by condensed zinc oxide, which begins to increase slowly at about 1600 K and subsequently very rapidly to a maximum value. Thereafter, the amount of zinc oxide decreases somewhat with temperature, while the amount of ZMFO increases. However, as room temperature is approached the amounts of ZMFO and zinc oxide decrease rapidly, while the amounts of zinc hydroxide carbonate ($Zn_5(OH)_6(CO_3)_2$), zinc hydroxide ($Zn(OH_2)$) and zinc carbonate ($ZnCO_3$) increase and at room temperature, zinc carbonate predominates.

Thermodynamically, as shown in Fig. 1 there would be very little zinc oxide and ZMFO at room temperature, but they are generally found in EAF dusts in considerable amounts, while typically zinc carbonate, zinc hydroxide and zinc hydroxide carbonate are rarely found to any great extent. The formation of the zinc carbonate, zinc hydroxide and zinc hydroxide carbonate would involve relatively low temperature gas–solid reactions and they would not be expected to form because of kinetic limitations. On the other hand, if the formation of these species could be promoted then this could potentially restrict or even eliminate the formation of the ZMFO. The deletion of zinc carbonate from the input, results in zinc hydroxide carbonate predominating at room temperature.

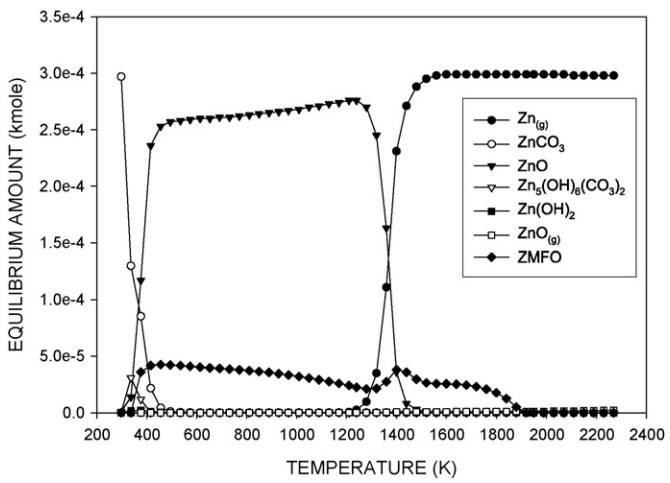

Fig. 1. The effect of temperature on the equilibrium amounts of zinc-containing species.

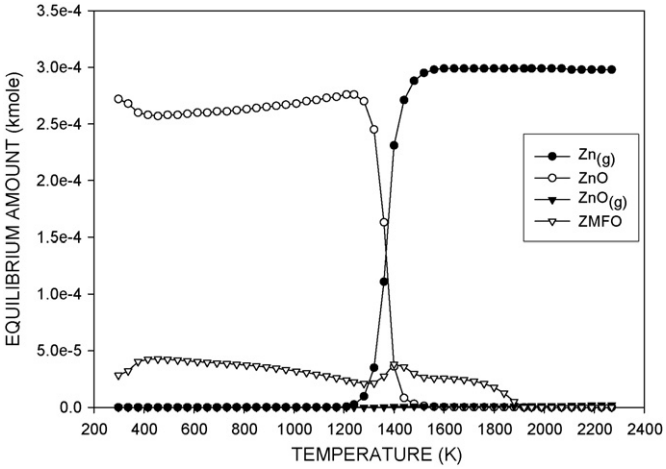

Fig. 2. The effect of temperature on the equilibrium amounts of zinc-containing species with zinc hydroxide, zinc hydroxide carbonate and zinc carbonate deleted.

Furthermore, the elimination of zinc hydroxide carbonate results in zinc hydroxide prevailing at room temperature. The results with all three of these species removed are shown in Fig. 2. In this case, the major zinc-containing species at room temperature would be zinc oxide and ZMFO. The general behaviors of the zinc oxide and ZMFO are similar to that exhibited in Fig. 1, except that as room temperature is approached the amount of ZMFO decreases somewhat and as a result the amount of zinc oxide increases. The effect of temperature on the equilibrium composition of the ZMFO is shown in Fig. 3. The spinel begins to form at about 1900 K and initially contains a large amount of iron and a small amount of manganese and is therefore mainly magnetite. As the temperature drops, the amount of iron decreases, while the amount of manganese increases. The amount of zinc begins to increase at about 1800 K and this corresponds to the decrease in the amount of zinc vapour (see Fig. 2). As the temperature drops even further, the amount of iron continues to decrease, while the amount of manganese peaks at about 1500 K and then decreases. Subsequently, the amount of zinc continues to increase and by about 1200 K the amounts of manganese and iron have become insignificant. Therefore, at room temperature, the ZMFO is mainly zinc ferrite as observed in many EAF dusts. Slow cooling of this dust would promote the formation of a zinc-rich ferrite, while a dust produced by rapid cooling would

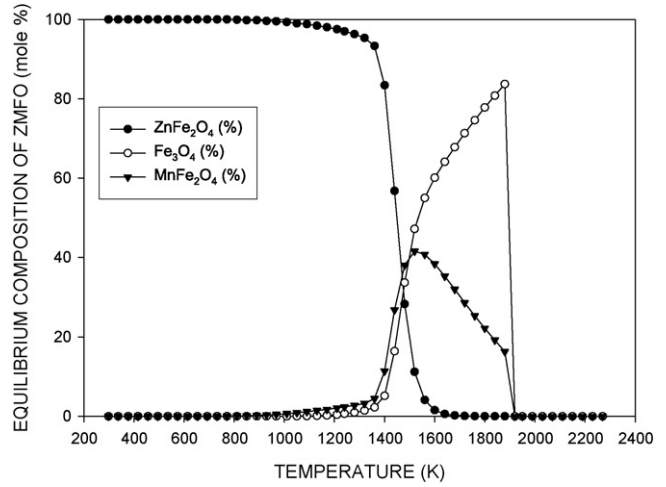

Fig. 3. The effect of temperature on the equilibrium composition of ZMFO with zinc hydroxide, zinc hydroxide carbonate and zinc carbonate deleted.

contain more iron and manganese. As shown in Fig. 3, at 1373 K for the standard conditions, the major component of the ZMFO is zinc and the iron and manganese contents are low. Therefore, this temperature was utilized in the determination of the effects of the variables on the formation of ZMFO in the subsequent calculations. Additionally, for the reasons mentioned above, zinc carbonate, zinc hydroxide and zinc hydroxide carbonate were not included in the ensuing calculations.

3.2. Effects of the amounts of zinc, manganese and iron

The effect of the amount of zinc in the dust on the amounts of ZMFO, zinc oxide, the iron oxides (sum of iron oxides) and the manganese oxides (sum of manganese oxides) at a temperature of 1373 K is shown in Fig. 4(a). The amount of ZMFO initially increases at low zinc levels, reaches a maximum and then decreases, while the amount of the iron oxides first decreases, reaches a minimum and then increases. Similarly, the amount of the manganese oxides first decreases and then increases. The amount of zinc oxide increases monotonically with the amount of zinc in the dust. These results are in general agreement with the characterization of actual EAF dusts where it has been observed that the amount of zinc ferrite in the dusts decreases with increasing zinc to iron ratio [8]. The equilibrium composition of the ZMFO is shown in Fig. 4(b). It can be seen that at low zinc additions, the amounts of zinc, manganese and iron increase in the spinel with increasing zinc. Subsequently, the manganese and iron levels reach maxima at a relatively low zinc level and then decrease. On the other hand, the zinc content of the spinel continues to increase and eventually reaches almost 100%. Fig. 4(c) shows the amount of ZMFO at three zinc levels of 1×10^{-4}, 3×10^{-4} and 5×10^{-4} kmol. It can be seen that at high temperatures, the amount of ZMFO is essentially independent of the zinc addition. Here the composition and the amount of ZMFO are mainly determined by the presence of the relatively large amounts of $MnFe_2O_4$ and Fe_3O_4, since the partial pressure of zinc vapour is high and there is very little $ZnFe_2O_4$. There is a significant minimum in the formation of ZMFO in the temperature range of about 1300–1400 K. This is due to the declining stabilities of $MnFe_2O_4$ and Fe_3O_4, but zinc vapour remains stable and thus ZMFO with a higher zinc ferrite content cannot form until lower temperatures are reached, where the zinc vapour is less stable. Subsequently, at even lower temperatures the amount of ZMFO increases, but the amount decreases with increasing zinc because of the higher stability of zinc oxide. Again as room temperature is approached the amount of ZMFO drops and the amount of zinc oxide increases.

As shown in Fig. 5(a), as the amount of manganese increases then the amount of the ferrite spinel decreases and ultimately disappears at the critical manganese content of about 2.25×10^{-4} kmol. The amounts of zinc oxide and the iron oxides increase as the ZMFO disappears and then level off, while the amount of the manganese oxides continuously increases. With regards to the ZMFO composition, as shown in Fig. 5(b), as the manganese increases then the zinc content drops while the manganese and iron contents slowly increase. However, at the critical manganese content of about 2.25×10^{-4} kmol, the zinc, manganese and the iron contents of the ferrite drop to zero as the ZMFO disappears. Fig. 5(c) shows the amount of ZMFO for three manganese levels of 1×10^{-4}, 3×10^{-4} and 5×10^{-4} kmol. It can be seen that the initial formation temperature of ZMFO shifts to lower temperatures with increasing manganese. Additionally, the amount of ZMFO at the lower temperatures is significantly reduced with increasing manganese in the dust. However, the low temperature formation of ZMFO would necessitate solid–solid reactions and because of kinetic reasons this would not be expected to occur to any great extent. Although the amount of ZMFO can be significantly reduced by manganese, the amounts required are much higher than typically present in EAF dusts.

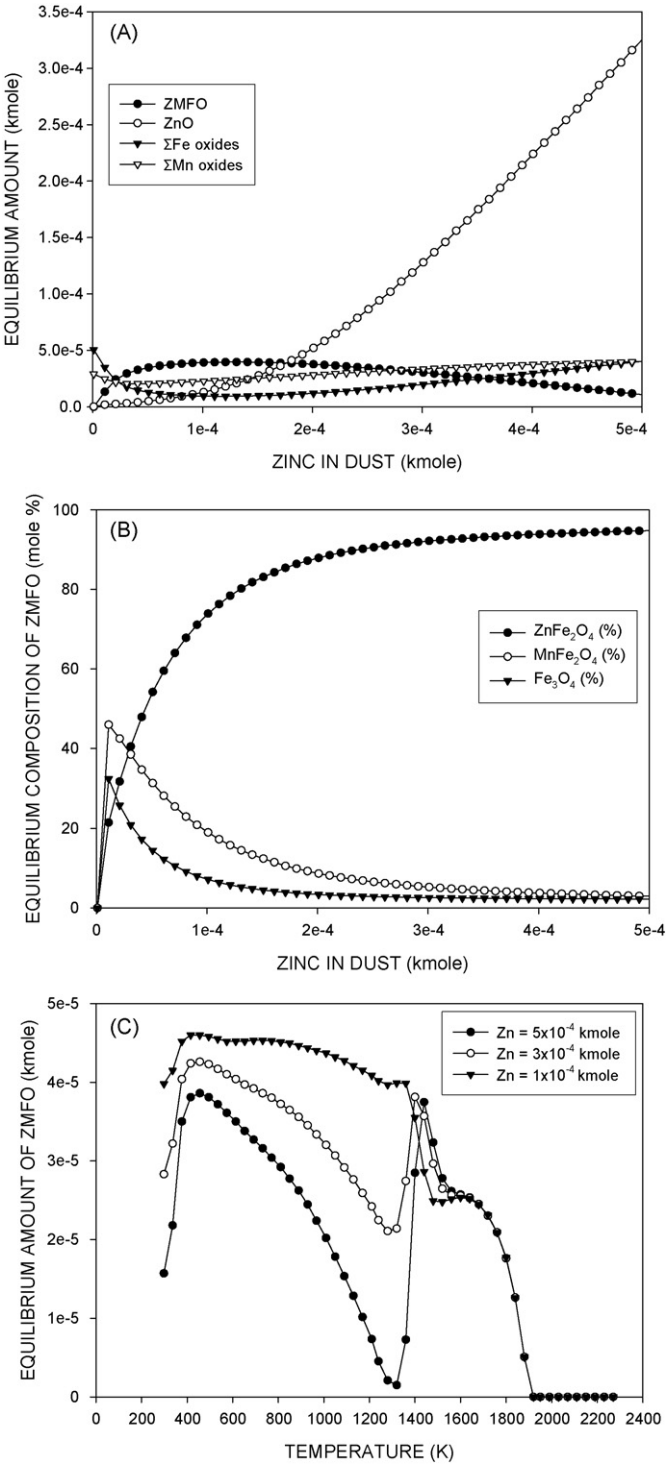

Fig. 4. Effect of zinc content of the dust: (A) the effect of zinc on the equilibrium amounts of zinc oxide, ZMFO, the iron oxides and the manganese oxides at 1373 K. (B) The effect of zinc on the equilibrium composition of the ZMFO at 1373 K. (C) The effect of temperature on the amount of ZMFO for three different zinc contents.

As shown in Fig. 6(a) at 1373 K an increasing amount of iron results in the formation of the ferrite spinel at an iron content of about 0.4×10^{-4} kmol and subsequently the amount of ZMFO increases and as a result the amount of zinc oxide decreases. The amount of the iron oxides increases upto the critical iron value and

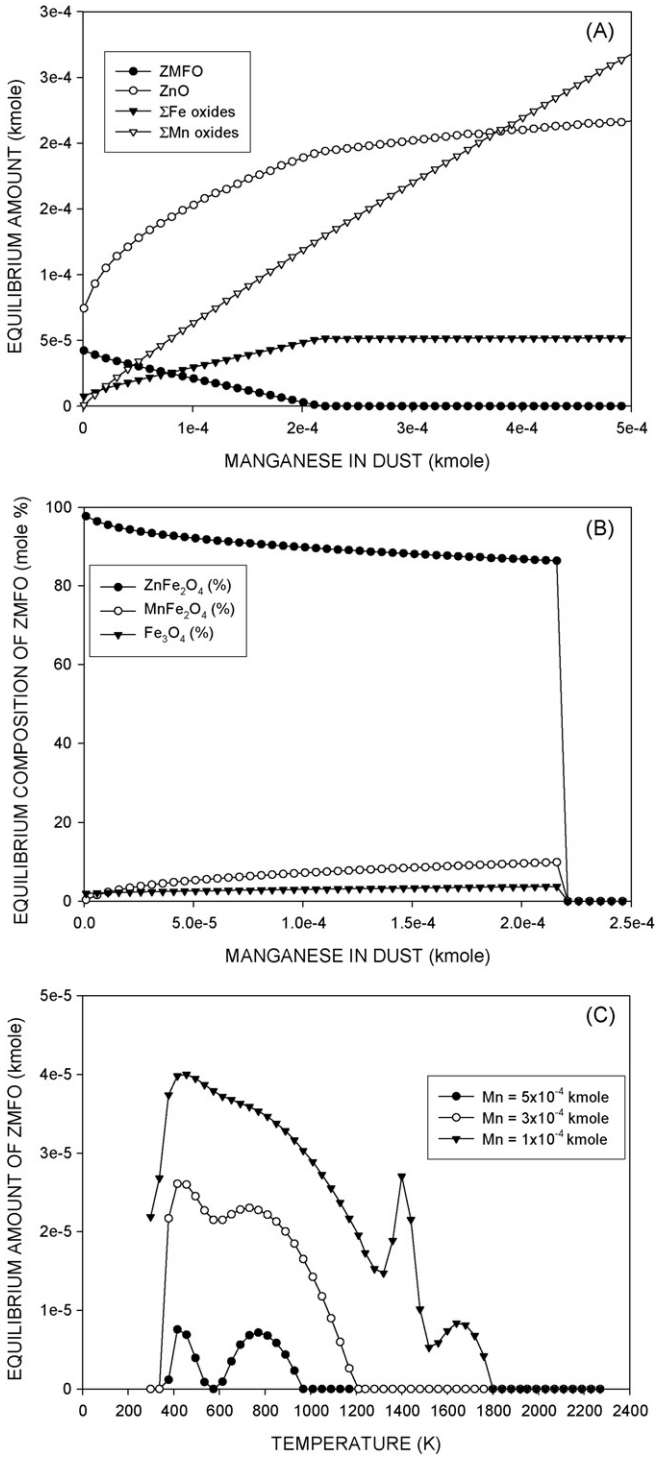

Fig. 5. Effect of manganese content of the dust: (A) the effect of manganese on the equilibrium amounts of zinc oxide, ZMFO, the iron oxides and the manganese oxides at 1373 K. (B) The effect of manganese on the equilibrium composition of the ZMFO at 1373 K. (C) The effect of temperature on the amount of ZMFO for three different manganese contents.

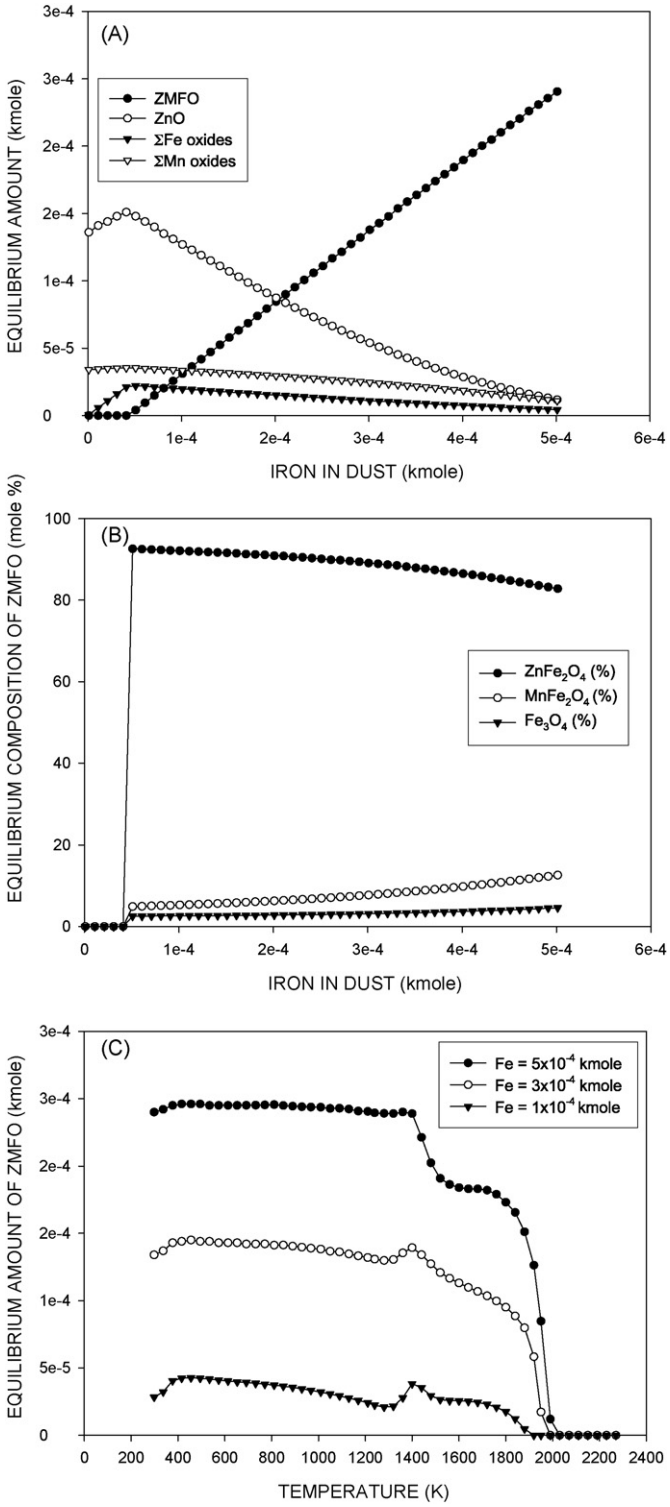

Fig. 6. Effect of iron content of the dust: (A) the effect of iron on the equilibrium amounts of zinc oxide, ZMFO, the iron oxides and the manganese oxides. (B) The effect of iron on the equilibrium composition of the ZMFO. (C) The effect of temperature on the amount of ZMFO for three different iron contents.

then decreases. On the other hand, the amount of the manganese oxides is constant upto the critical iron value and then decreases. With regards to the composition, as shown in Fig. 6(b), with increasing iron, the zinc content increases rapidly as the first ZMFO forms then decreases slowly. Similarly, the iron and manganese contents increase rapidly as the first ZMFO forms and continue to increase with increasing iron. Fig. 6(c) shows the effect of temperature on the amount of ZMFO for various iron additions. It can be seen that an increasing amount of iron favours the formation of ZMFO and promotes the formation of the ZMFO at higher temperatures. The increasing formation of ZMFO with increasing iron is mainly due to the availability of zinc oxide.

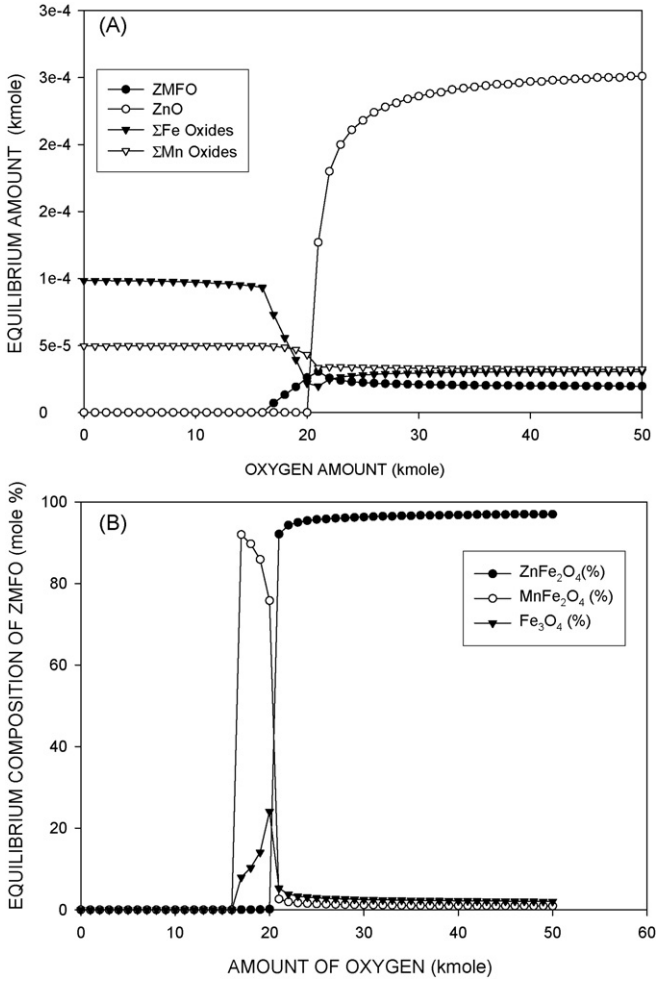

Fig. 7. Effect of amount of oxygen in the gas phase at 1373 K on: (A) the equilibrium amounts of zinc oxide, ZMFO, the iron oxides and the manganese oxides. (B) The equilibrium composition of the ZMFO.

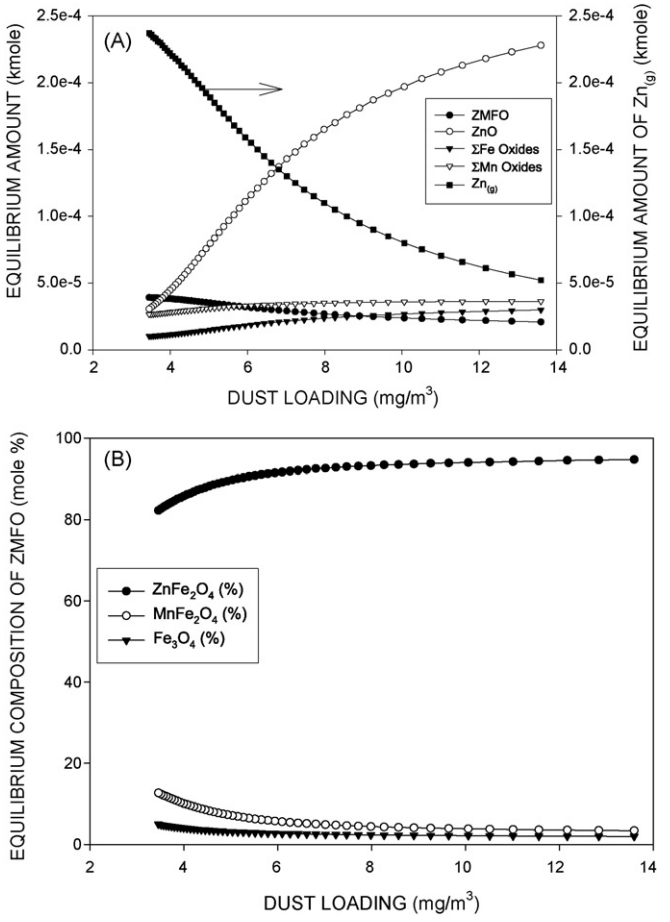

Fig. 8. Effect of dust loading in the gas phase at 1373 K on: (A) the equilibrium amounts of zinc oxide, ZMFO, the iron oxides and the manganese oxides. (B) The equilibrium composition of the ZMFO.

3.3. Effects of oxygen potential and dust loading

Another factor affecting the amount and the composition of the ZMFO is the oxygen potential of the atmosphere. Again a temperature of 1373 K was selected. Fig. 7(a) shows that at low oxygen contents and therefore oxygen potential there is no ZMFO. However, this very low oxygen potential would be difficult to achieve in an electric arc furnace atmosphere. As the amount of oxygen increases further, the spinel forms very quickly, reaches a maximum, then decreases slightly and becomes essentially independent of the amount of oxygen. Zinc oxide develops very rapidly after the ZMFO has formed. The iron and the manganese oxides are essentially independent of the amount of oxygen but exhibit a large decrease as the ZMFO forms. The composition of the ZMFO is shown in Fig. 7(b). At an oxygen addition of about 17 kmol, the iron content increases rapidly, reaches a maximum at about 20 kmol and then decreases. Similarly the manganese content also increases, peaks and decreases. Subsequently, both the manganese and the iron essentially disappear and zinc ferrite predominates at high oxygen additions. This sequence again represents the higher stability of the zinc-rich ferrite and demonstrates that in most dusts the ZMFO will mainly consist of zinc ferrite, particularly at room temperature and with relatively slow cooling of the dust particles in a high oxygen potential atmosphere.

The effect of dust loading was investigated by varying the amount of nitrogen gas at 1373 K and the results for the amounts of the various species are shown in Fig. 8(a). The amount of ZMFO increased with decreasing dust loading, while the amounts of zinc oxide and the iron and manganese oxides decreased. Fig. 8(a) also shows the amount of zinc vapour and it can be seen that the amount of gaseous zinc increases with decreasing dust loading as a result of the lowered partial pressure of zinc. This lowers the amount of zinc oxide but the amount of ZMFO increases. Also as shown in Fig. 8(b), the amount of zinc in the ZMFO decreases with decreasing dust loading and as a consequence, the amounts of iron and manganese increase.

3.4. Effect of calcium oxide

Another major constituent of the dust is calcium oxide (CaO). The addition of calcium oxide results in the following additional species in the equilibrium calculation: calcium oxide (CaO), calcium carbonate ($CaCO_3$), calcium hydroxide ($Ca(OH)_2$), calcium ferrite ($CaO{\cdot}Fe_2O_3$), dicalcium ferrite ($2CaO{\cdot}Fe_2O_3$), calcium triiron pentoxide ($CaFe_3O_5$) and calcium pentairon heptaoxide ($CaFe_5O_7$). Fig. 9(a) shows the effect of temperature on the zinc and calcium oxide-containing species as a function of temperature for a calcium oxide addition of 1×10^{-4} kmol. It can be seen that under the equilibrium conditions and in the presence of calcium oxide, ZMFO should only form at relatively low temperatures due to the higher stabilities of the calcium ferrites at the higher temperatures. Again, the formation of ZMFO at such low temperatures via solid-state reactions would be unlikely and this again indicates that the ZMFO in actual dusts forms at much higher temperatures and equilib-

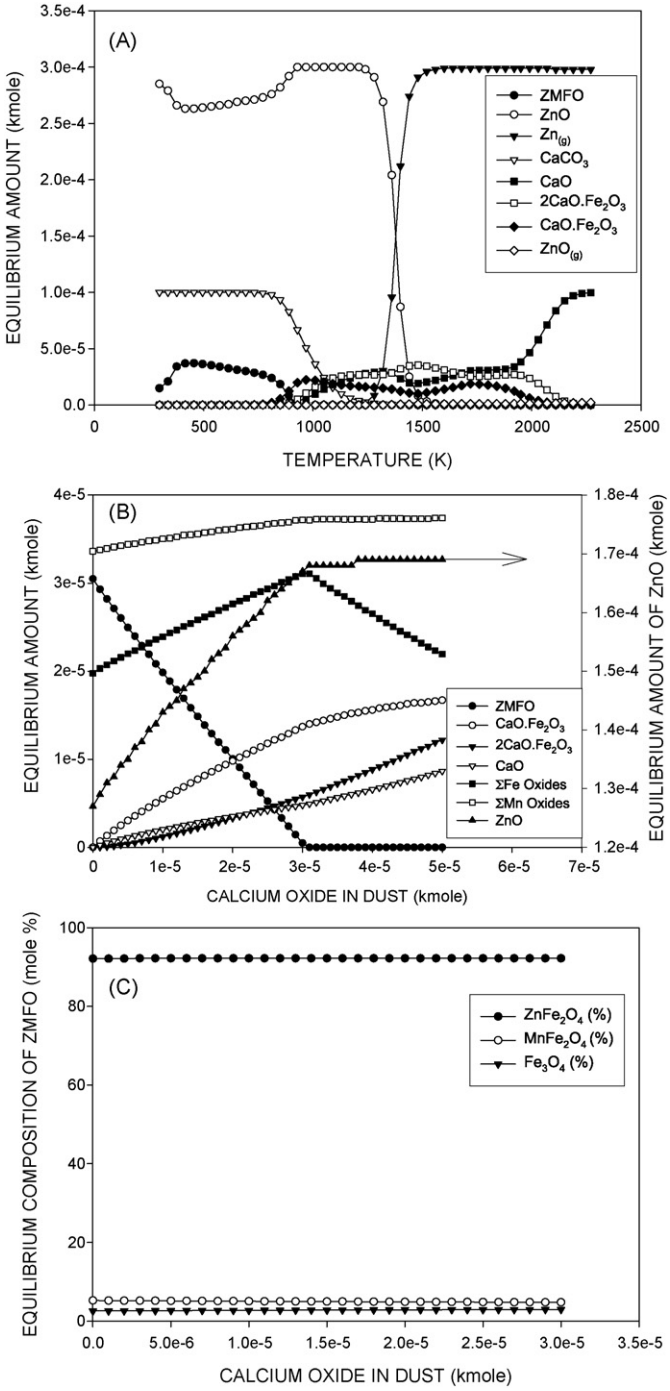

Fig. 9. Effect of calcium oxide in the dust on: (A) the zinc and calcium-containing species as a function of temperature. (B) The equilibrium amounts of zinc oxide, ZMFO, the iron oxides and the manganese oxides at 1373 K. (C) The equilibrium composition of the ZMFO at 1373 K.

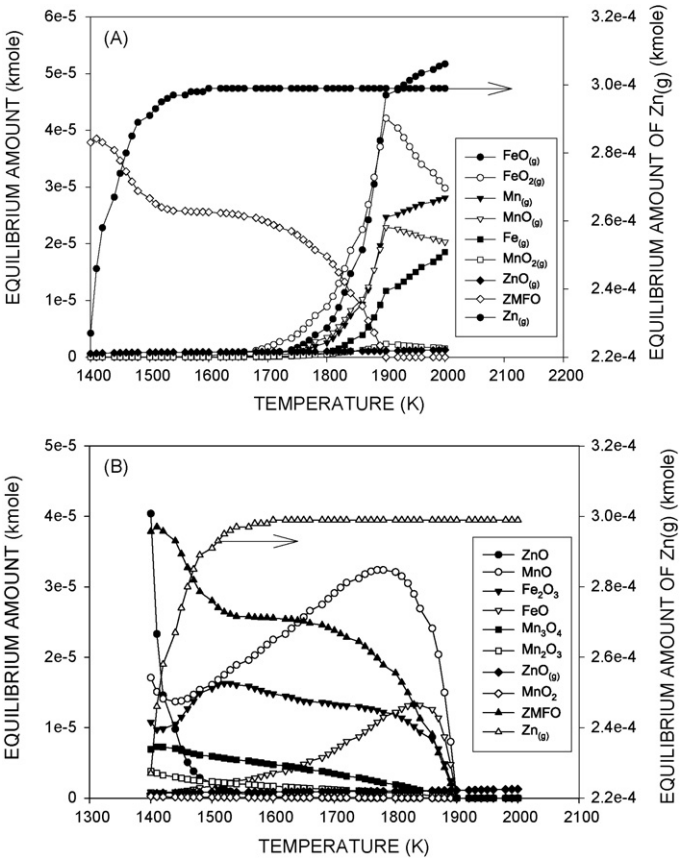

Fig. 10. Effect of temperature on the amounts of: (A) the zinc, manganese and iron-containing gaseous species in equilibrium with ZMFO. Zinc vapour is also included. (B) The condensed zinc, manganese and iron oxide species in equilibrium with ZMFO. Zinc vapour is also included.

rium is not achieved during the cooling of the dust. Furthermore, although some calcium carbonate can be found in EAF dusts there is usually a relatively large proportion of calcium oxide, which under equilibrium conditions is only stable at high temperatures. Once more this indicates that the dust does not reach equilibrium and the actual dust composition at room temperature more closely resembles the equilibrium composition at much higher temperatures.

Fig. 9(b) shows the amounts of the calcium-containing species, the iron and manganese oxides, ZMFO and zinc oxide at 1373 K as a function of the calcium oxide addition. An increasing amount of calcium oxide results in a decrease in the amount of the ZMFO as the formation of the calcium ferrites ($CaO{\cdot}Fe_2O_3$ and $2CaO{\cdot}Fe_2O_3$) is more favourable. Correspondingly, this results in the liberation of zinc oxide and iron oxide until all of the ferrite spinel has disappeared at a calcium oxide addition of about 3×10^{-5} kmol. Then, the amount of zinc oxide remains relatively constant but the amount of iron oxide decreases as the amounts of the calcium ferrites continue to increase. In actual EAF dusts the amount of calcium ferrite is relatively low despite relatively large amounts of calcium oxide and again this likely reflects the relative slowness of a reaction involving solid calcium oxide. As shown in Fig. 9(c), at 1373 K, the composition of the ferrite spinel does not change with increasing calcium oxide addition.

4. Mechanism of formation of ZMFO ($(Zn_xMn_yFe_{1-x-y})Fe_2O_4$)

The formation of the ZMFO involves a reaction between oxygen, zinc, manganese and iron. Fig. 10(a) shows the amounts of the gaseous species in the Fe–Mn–Zn–O system that are in equilibrium with the ZMFO from 1400 to 2000 K. Manganese and iron metallic vapours and iron and manganese monoxide vapours disappear by about 1700 K. On the other hand, iron dioxide exists down to about 1600 K. At steelmaking temperatures of 1873 K, the amounts of the gaseous iron and manganese species would be expected to be relatively small and the temperatures of the gas in the freeboard of the furnace would be expected to be much lower than that of the melt. Therefore it is more likely that the ZMFO forms at lower temperatures where both condensed iron and manganese oxides and

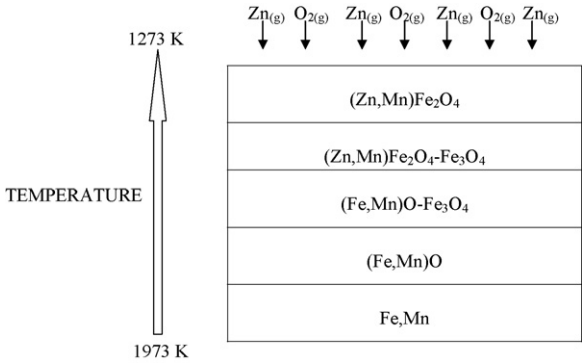

Fig. 11. Proposed oxidation reaction sequence on the surface of an iron–manganese. Particle in contact with both gaseous zinc and oxygen in the atmosphere above the melt in an electric arc furnace.

zinc vapour are stable. The ZMFO could form from the oxidation of manganese-containing iron particles. Fig. 10(b) shows the amounts of the iron and manganese oxides, the ZMFO, zinc oxide and gaseous zinc. It can be seen that both FeO and MnO begin to form at about the same temperature as the initial formation temperature of the ZMFO and once the spinel begins to form then their amounts decrease. Again this ZMFO would be enriched in iron and manganese. Zinc vapour remains stable even after considerable ZMFO has formed and thus the zinc content of the ZMFO is relatively low until lower temperatures are reached.

Fig. 11 shows a schematic diagram of the proposed reaction mechanism for the oxidation of a manganese-containing iron particle, with the composition of the oxide changing as the temperature decreases. Initially, the oxide on the iron–manganese particle would be (Fe, Mn)O but as the temperature drops then some Fe_3O_4 would form. As the temperature drops even further and the particle begins to react with the zinc vapours then some (Zn, Mn)Fe_2O_4 would appear with the Fe_3O_4. Subsequently after further reaction with zinc vapour then ZMFO ($(Zn_xMn_yFe_{1-x-y})Fe_2O_4$) would be produced. This explanation would be consistent with the findings of Li and Tsai [27]. From a thermodynamic perspective and as shown in the Figure, as the temperature drops to room temperature, the amount of zinc in the ZMFO should increase but depending on the cooling rate, the actual dust composition may more closely reflect the composition of the ZMFO at the higher temperatures.

5. Conclusions

1. The formation of the ZMFO ($(Zn_xMn_yFe_{1-x-y})Fe_2O_4$) in electric arc furnace dust was investigated using the equilibrium module of HSC Chemistry® 6.1 and methods for mitigating its formation were studied. In general it was found that the composition of actual EAF dusts more closely represents that formed at high temperatures and therefore equilibrium is not achieved as the dust cools to room temperature.
2. For the gas composition used, the thermodynamic calculations show that at room temperature, zinc oxide and ZMFO are not stable due to the higher stability of zinc hydroxide, zinc hydroxide carbonate and zinc carbonate. However, the formation of these species is kinetically not favourable and if they are eliminated as possible stable species then zinc oxide and ZMFO predominate at room temperature. This composition more closely resembles that of actual dusts. Slow cooling of the dust would lead to a zinc-rich ferrite, while rapid cooling would produce a ferrite with relatively high levels of iron and manganese.
3. The amount of ZMFO at room temperature generally decreases with increasing zinc and manganese in the dust. On the other hand the amount of ZMFO increases with increasing iron.
4. ZMFO can be eliminated by reducing the oxygen potential at 1373 K, but this requires relatively low oxygen potentials, which would not be easily attained in an electric arc furnace. Additionally, the amount of ZMFO decreases with increasing dust loading.
5. Thermodynamically, the presence of calcium oxide can reduce the amount of ZMFO at 1373 K, through the formation of the various calcium ferrites. However, despite a relatively large amount of calcium oxide in many EAF dusts this effect is not significant and this is attributed to the slow kinetics of the reactions involving solid calcium oxide.
6. It is proposed that the ZMFO is formed by the sequential oxidation of iron-containing manganese particles in the presence of zinc vapour as follows, with decreasing temperature; Fe–Mn, (Fe, Mn)O, (Fe, Mn)O–Fe_3O_4, (Zn, Mn)Fe_2O_4–Fe_3O_4, $(Zn_xMn_yFe_{1-x-y})Fe_2O_4$.

Acknowledgements

The author thanks the Natural Sciences and Engineering Research Council of Canada for the support of this research.

References

[1] J.-C. Huber, P. Rocabois, M. Faral, J.P. Birat, F. Patisson, D. Ablitzer, The formation of EAF dust, in: Electric Furnace Conference Proceedings, vol. 58, Iron and Steel Society of AIME, Warrendale, PA, 2000, pp. 171–181.
[2] R.S. Badger, W.A. Kneller, Characterization and formation of electric arc furnace (EAF) dusts, in: Electric Furnace Conference Proceedings, vol. 55, Warrendale, PA, Iron and Steel Society of AIME, 1997, pp. 95–98.
[3] A.-G. Guezennec, J.-C. Huber, F. Patisson, P. Sessiecq, J.P. Birat, D. Ablitzer, Dust Formation in electric arc furnace: birth of the particles, Powder Technology 157 (1–3) (2005) 2–11.
[4] L.M. Southwick, Commercializing EAF dust treatment technologies: regulatory and process design impacts, in: I. Gaballah, J. Hager, R. Solozabal (Eds.), REWAS'99—Global Symposium on Recycling, Waste Treatment and Clean Technology, Proceedings, San Sebastian, Spain, September 5–9, 1999, vol. 1, The Minerals Metals Materials Society, Warrendale, PA, 1999, pp. 311–325.
[5] C.A. Moraes, F.A. Brehm, State of art of electric arc furnace dust recycling, in: Seminario de Aciaria—Internacional, 38th, Belo Horizonte, Brazil, May 20–23, 2007, Associacao Brasileira de Metalurgia e Materiais, Sao Paulo, Brazil, 2007, pp. 90–100.
[6] A.D. Zunkel, Electric arc furnace dust management: a review of technologies, Iron and Steel Engineer 74 (3) (1997) 33–38.
[7] J.G.M.S. Machado, F.A. Brehm, C.A.M. Moraes, C.A. Dos Santos, A.C.F. Vilela, J.B. Marimon da Cunha, Chemical, physical, structural and morphological characterization of the electric arc furnace dust, Journal of Hazardous Materials 136 (3) (2006) 953–960.
[8] J.G.M.S. Machado, F.A. Brehm, C.A.M. Moraes, C.A. Dos Santos, A.C.F. Vilela, J.B. Marimon da Cunha, Characterization study of electric arc furnace dust phases, Materials Research (Sao Carlos, Brazil) 9 (1) (2006) 41–45.
[9] F.M. Martins, J. Manoel dos Reis Neto, C. Jorge da Cunha, Mineral phases of weathered and recent electric arc furnace dust, Journal of Hazardous Materials 154 (1–3) (2008) 417–425.
[10] T. Sofilic, A. Rastovcan-Mioc, S. Cerjan-Stefanovic, V. Novosel-Radovic, M. Jenko, Characterization of steel mill electric-arc furnace dust, Journal of Hazardous Materials 109 (1–3) (2004) 59–70.
[11] A.M. Hagni, R.D. Hagni, C. Demars, Mineralogical characteristics of electric arc furnace dusts, JOM 43 (4) (1991) 28–30.
[12] A.M. Hagni, R.D. Hagni, Reflected light and scanning electron microscopic study of electric arc furnace (EAF) dusts, in: R.G. Reddy, W.P. Imrie, P.B. Queneau (Eds.), Residues Effluents: Processing and Environmental Considerations, Proceedings of International Symposium, The Minerals Metals Materials Society, Warrendale, PA, 1992, pp. 117–125.
[13] R.D. Hagni, A.M. Hagni, Process mineralogy of lead smelter and electric arc furnace dusts, in: W. Petruk, A.R. Rule (Eds.), Process Mineral, XII, The Minerals Metals Materials Society, Warrendale, PA, 1994, pp. 355–365.
[14] T.T. Chen, J.E. Dutrizac, D.R. Owens, Mineralogical characterization of EAF dusts from plain carbon steel and stainless steel operations, in: S.R. Rao (Ed.), Waste Processing and Recycling in Mineral and Metallurgical Industries III, Calgary, Alberta, August 16–19, 1998, Canadian Institute of Mining, Metallurgy and Petroleum, Montreal, Quebec, 1998, pp. 511–525.
[15] A.F. Ellis, J. Glover, Mechanism of fume formation in oxygen steel making, Journal of the Iron and Steel Institute 209 (Pt. 8) (1971) 593–599.
[16] A.G. Guezennec, F. Patisson, P. Sessiecq, J.C. Huber, D. Ablitzer, Modeling dust evolution in electric arc furnace (EAF) fume extraction system, in: F. Kongoli, R.G. Florian, Reddy (Eds.), Advanced Processing of Metals and Materials, Sohn International Symposium, Proceedings, San Diego, CA, August 27–31, 2006, vol. 5, The Minerals Metals Materials Society, Warrendale, PA, 2006, pp. 241–250.

[17] J.C. Huber, F. Patisson, P. Rocabois, J.-P. Birat, D. Ablitzer, Some means to reduce emissions and improve the recovery of electric arc furnace dust by controlling the formation mechanisms, in: I. Gaballah, J. Hager, R. Solozabal (Eds.), REWAS'99—Global Symposium on Recycling, Waste Treatment and Clean Technology, Proceedings, San Sebastian, Spain, September 5–9, 1999, vol. 2, The Minerals Metals Materials Society, Warrendale, PA, 1999, pp. 1483–1492.
[18] P. Rocacbois, J.-C. Huber, E. Lectard, F. Patisson, Thermodynamic assessment of the oxide phases in the Fe–Zn–O system—application to dust formation in electric arc furnace, Energietechnik/Energy Technology (Pt. 1, High Temperature Materials Chemistry, Part 1) 15 (2000) 249–252.
[19] M. Olette, M.F. Ancey-Moret, Diagrams showing the relative values of vapor pressure and heat contents of elements, Vide 22 (130) (1967) 213–225.
[20] L. von Bogdandy, H.D. Pantke, The dust produced during blowing in the converter as an indicator of the refining process when using oxygen-enriched air, Stahl und Eisen 78 (1958) 792–798.
[21] M.J. Thomson, N.G. Kournetas, E. Evenson, I.D. Sommerville, A. McLean, J. Guerard, Effect of oxyfuel burner ratio changes on energy efficiency in electric arc furnace at co-steel lasco, Ironmaking and Steelmaking 28 (3) (2001) 266–272.
[22] A. Roine, Chemical Reaction and Equilibrium Software with Thermochemical Database and Simulation Module, HSC Chemistry® 6.1, Outotec Research Oy, Pori, Finland, 2007.
[23] J.C. Vuillermoz, J. Laurent, S. Bockel-Macal, F. Januard, B. Allemand, Measurement of Gas Components Contained in the Flue Gas of Furnaces, Fr. Demande, 2005, 19 pp.
[24] M.N. Kaibicheva, Dust formation in electric furnace during oxygen blowing, Stal 20 (1960) 809–812.
[25] F. Harms, W. Riemann, Measuring the waste gas and dust quantities of a 70-ton electric arc furnace operating partly with oxygen, Stahl und Eisen 82 (1962) 1345–1348.
[26] M. Nakayama, H. Kubo, Progress of emission control system in electric arc furnace melt-shops, NKK Technical Review, no. 84 (2001) 16–23.
[27] C.L. Li, M.S. Tsai, Mechanism of spinel ferrite dust formation in Electric arc furnace steelmaking, ISIJ International 33 (2) (1993) 284–290.